Constructing Ionospheric Irregularity Threat Model for Korean SBAS

Eugene Bang, Jinsil Lee, and Jiyun Lee
Korea Advanced Institute of Science and Technology

Jiwon Seo
Yonsei Unversity

Todd Walter
Stanford University

BIOGRAPHY

Eugene Bang received his B.S. in Aerospace Engineering from Korea Aerospace University in 2010. He is currently a Ph.D. student in the Department of Aerospace Engineering at Korea Advanced Institute of Science and Technology (KAIST). His research interests include GNSS augmentation system and Receiver Autonomous Integrity Monitoring (RAIM).

Jinsil Lee received her B.S. in Civil and Environmental Engineering from Korea Advanced Institute of Science and Technology (KAIST) in 2012. She is currently a Ph.D student in the Department of Aerospace Engineering at KAIST. Her research interests include GNSS augmentation system and space weather forecasting for GNSS application.

Jiyun Lee is an Assistant Professor in department of Aerospace Engineering at Korea Advanced Institute of Science and Technology. She has supported the GBAS and SBAS program over the past eight years a consulting professor at Stanford University and a Principal GPS Systems Engineer at Tetra Tech AMT. She received her Ph.D. from Stanford University (2005) in aeronautics and astronautics. Prior to joining AMT, she worked for SiRF Technology, Inc. as a Senior GPS systems engineer. She has been active in the Institute of Navigation (ION), serving as Session co-Chair and Track Chair.

Jiwon Seo is an Assistant Professor in the School of Integrated Technology at Yonsei University. He received his B.S degree in mechanical engineering (division of aerospace engineering) from KAIST and received M.S. degrees in aeronautics/astronautics and electrical engineering from Stanford University and a Ph.D. degree in aeronautics/astronautics from Stanford University in 2010. His research interests include GPS anti-jamming technology and Alternative Position Navigation and Timing (APNT) technology such as eLoran.

Todd Walter is a Senior Research Engineer in the Department of Aeronautics and Astronautics at Stanford University. He received his Ph.D. in 1993 from Stanford University. His current activities include defining future architectures to provide aircraft guidance and working with the FAA on the implementation of dual-frequency WAAS. Key early contributions include: prototype development proving the feasibility of WAAS, significant contribution to WAAS MOPS, and design of integrity algorithms for WAAS. He is a fellow of the ION and served as its president.

ABSTRACT

Single-frequency based Satellite-Based Augmentation Systems (SBAS), the augmentation of the Global Navigation Satellite System (GNSS), broadcast estimates of vertical ionospheric delays and confidence bounds on the delay errors at Ionospheric Grid Points (IGPs). Using an ionospheric irregularity undersampled threat model, the integrity bounds, called Grid Ionospheric Vertical Errors (GIVEs), must be augmented to bound ionospheric irregularity threats which may exist between or beyond Ionospheric Pierce Points (IPPs) under ionospheric storm conditions. Since the ionospheric disturbed conditions can vary significantly from one region to another region, threat models need to be built for regions where SBAS will be operational. This paper presents a new method for constructing an undersampled threat model for SBAS in the Korean region, examines the influence of threat model to system availability, and demonstrates the performance of a newly developed threat model.

The existing method tabulates undersampled threats in the threat model as a function of two metrics which measure the density and uniformity of IPP distribution in a region. Thus, the threat model metrics, which characterize threatening undersampled geometries including the density of IPP distribution accurately, play a critical role in improving system performance. The first threat metric,

fit radius, is defined by an IPP search method used for a planar fit algorithm. This paper first determines a range of the fit radius optimized for the Korean region by considering the ionospheric observability and quality of the planar fit. Next this paper proposes a new second metric, the Relative Bin Number (RBN) metric, alternative to the Relative Centroid Metric (RCM) currently used in WAAS. RBN is more effective than the existing threat metric in capturing the sparseness of the IPP distribution by measuring the ratio of the number of partitions in which IPPs are absent to the total number of partitions. In addition, other essential parameters for the Korean SBAS threat model construction, including GEO MT28 (Message Type 28), IGP formations, and the number of reference stations, are determined. In a preliminary assessment, the undersampled ionospheric threat model based on the new methodology increased the coverage of 99.9% availability for APV-I service from 18.48% to 91.10%.

1.0 INTRODUCTION

The ionosphere is one of the largest and most unpredictable error sources which may degrade the accuracy and integrity of single-frequency-based GNSS augmentation systems. Satellite Based Augmentation Systems (SBAS) broadcast to users both estimates of ionospheric delays on Ionospheric Grid Points (IGPs) and the confidence bounds on the error of these delay estimates, called the Grid Ionospheric Vertical Errors (GIVEs). Under nominal conditions, these integrity bounds are mainly based on the formal error variance of the delay estimates associated with measurement noise and the uncertainty of planar fits. However, during ionospheric storms, small-scale irregularities may form in the ionosphere, and result in erroneous delay estimates if not observed by SBAS reference stations Thus, the GIVE must be augmented to protect users against the threats arising from undersampled ionospheric irregularities by developing an ionospheric threat model.

Ionospheric behaviors under highly disturbed conditions significantly vary in each region. Thus, it is essential to understand the characteristics of ionospheric irregularities and define the threats associated with undersampled disturbances where SBAS will become operational. The worst-case threats associated with undersampled irregularities are simulated using “data deprivation” methodologies [1]. The deprivation schemes exclude single ionospheric pierce point (IPP) or a set of IPPs from the computation of a planar fit. Potential undersampled threats are estimated based on the residuals between planar fit estimates and user measurements at IPPs. Those threats are characterized by two threat model metrics that work as a measure of the density or uniformity of IPPs in the region around each IGP. The error variances that protect users from the undersampled threats are tabulated in the threat model as a function of those metrics and augment the computation of GIVE values.

The first threat metric, planar fit radius, measures the density of IPP distribution and more importantly defines a fit domain where IPPs to be used in the planar fit are selected. In fact, the IPP search algorithm determines the fit radius corresponding to each planar fit at the IGP and the fit domain defined by the fit radius has an impact on the quality of the planar fit. Moreover, regional ionospheric observability was considered in the original IPP search algorithm used for the Wide Area Augmentation System (WAAS), a SBAS developed by the U.S. Federal Aviation Administration (FAA), or the Multi-functional Satellite Augmentation System (MSAS), which is the Japanese SBAS. Thus, to construct the Korean ionospheric threat model, we need to modify parameter criteria for IPP selection and the method of searching available IPPs in the region surrounding the IGP.

Poorly designed metrics, especially in terms of the second threat metric, may apply worse error variances than needed to less vulnerable IPP geometries [3]. This leads to overconservative GIVE values and thus reduces system availability. Therefore, the threat model metrics that accurately characterize threatening undersampled geometries are critical in improving the performance of SBAS. The threat model of WAAS uses the Relative Centroid Metric (RCM) as a measure of the IPP distribution [4]. This metric cannot make a distinction between different IPP geometries if especially those have a symmetric IPP distribution. The Maximum Separation Angle (MSA) metric proposed for MSAS measures the maximum angle between adjacent IPPs to determine the skewness of the IPP distribution [5]. However, the MSA consider IPP geometries with multiple large angles to be no worse than those with single large angle if the magnitudes of the maximum angle are identical. In this paper, we propose a new metric for the Korean SBAS threat model which effectively subdivides the cases of IPP distribution.

This paper constructs an undersampled ionospheric threat model for SBAS in the Korean region, and demonstrates the performance of the threat model by assessing the availability of the single-frequency SBAS on the Korean peninsula. We also investigate how the number and location of SBAS reference stations affect system availability. Section 2.0 introduces the dual-frequency GPS data and SBAS reference station candidates used to construct undersampled ionospheric threat model. In Section 3.0, the methodology of undersampled threat model construction for a future SBAS in Korean region and the resulting threat model is presented. Section 4.0 discusses the results of availability simulation performed

using the derived threat model. This study is concluded in Section 5.0 with remarks for future work.

2.0 DATA

To identify ionospheric irregularity threats which may escape detection, we analyze precise ionospheric delay estimates generated by a simplified truth processing method [6-8]. Dual-frequency GPS observables are collected from 74 nationwide GPS reference stations in South Korea. Data from a total of 22 days on which moderate to extreme ionospheric storms occurred during the last solar maximum period (2000 – 2004) are processed to compute the ionospheric delay estimates. The values of planetary K-index (Kp) and *disturbance, storm time* (Dst) are used to target days on which ionospheric irregularities were likely to have occurred. The dates whose Kp is greater than 6 or the magnitude of Dst is larger than 200 are selected and listed in Table 1.

Table 1. Ionospheric storm dates during the last solar peak in 2000 - 2004.

Day (UT mm/dd/yyyy)	Dst	Kp	Geomagnetic Storm Class
04/06/2000	-287	8.3	Severe
04/07/2000	-288	8.7	Extreme
07/15/2000	-289	9.0	Extreme
07/16/2000	-301	7.7	Strong
08/12/2000	-235	7.7	Strong
09/17/2000	-201	8.3	Severe
03/31/2001	-387	8.7	Extreme
04/01/2001	-228	5.7	Moderate
04/11/2001	-271	8.3	Severe
04/12/2001	-236	7.3	Strong
11/06/2001	-292	8.7	Extreme
11/24/2001	-221	8.3	Severe
09/07/2002	-177	7.3	Strong
10/29/2003	-350	9.0	Extreme
10/30/2003	-383	9.0	Extreme
10/31/2003	-307	8.3	Severe
11/20/2003	-422	8.7	Extreme
11/21/2003	-309	6.7	Moderate
07/17/2004	-76	6.0	Moderate
11/08/2004	-374	8.7	Extreme
11/09/2004	-214	8.7	Extreme
11/10/2004	-263	8.7	Extreme

Figure 1 shows the Korean GNSS reference station networks that are operated by the DGPS Central Office (DCO), the National Geographic Information Institute (NGII), and the Korea Astronomy and Science Institute (KASI). Of those stations (74 as of 2004), the National Differential GPS (NDGPS) reference stations operated by DCO [9] are likely to be used as SBAS monitor stations if deployed in future. Considering the geographical distribution of stations and a SBAS service volume, seven domestic NDGPS stations are selected to form the SBAS monitor station network in this study. The chosen reference stations marked in red triangle with four-character station ID are shown in Figure 1 and listed in Table 2.

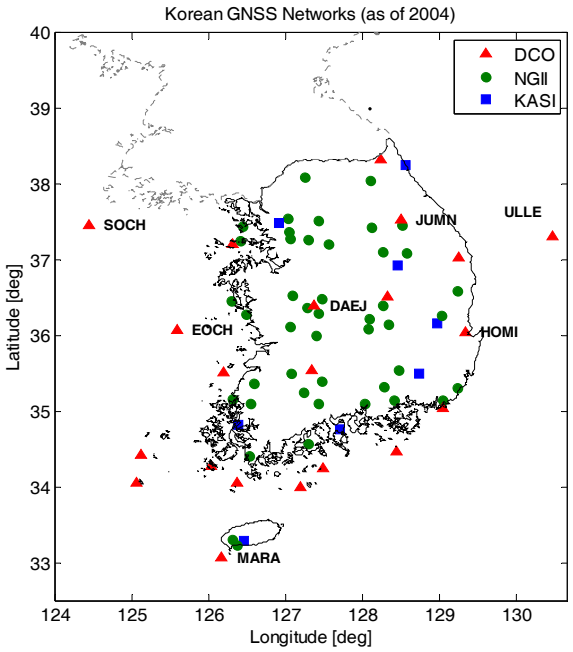

Figure 1. Korean GNSS reference station networks. Red triangles with station ID indicate 7 NDGPS stations selected as SBAS reference station candidates.

Table 2. Korean NDGPS stations considered as SBAS reference station candidates

No.	Mountpoint	Data Format	Navigation Service
1	DAEJ_RTCM20	RTCM 2.0	DGPS
	DAEJ_RTCM23	RTCM 2.3	DGPS+RTK
2	SOCH_RTCM20	RTCM 2.0	DGPS
3	JUMN_RTCM20	RTCM 2.0	DGPS
4	MARA_RTCM20	RTCM 2.0	DGPS
	MARA_RTCM23	RTCM 2.3	DGPS+RTK
5	HOMI_RTCM20	RTCM 2.0	DGPS
6	EOCH_RTCM20	RTCM 2.0	DGPS
	EOCH_RTCM23	RTCM 2.3	DGPS+RTK
7	ULLE_RTCM20	RTCM 2.0	DGPS

3.0 UNDERSAMPLED IONOSPHERIC IRREGULARITY THREAT MODEL

3.1 Methodology of Threat Model Construction

To construct an undersampled ionospheric irregularity threat model, the existing methodologies including planar fit and data deprivation techniques [10] are used in this

study. As for the data deprivation, single station deprivation and malicious deprivation schemes [1-3][11] , originally designed to construct the WAAS ionospheric threat model, are used to simulate the worst-case threats due to undersampling. A planar fit is constructed using a set of slant ionospheric delay measurements observed at SBAS reference stations. The deprivation schemes exclude single ionospheric pierce point (IPP) or a set of IPPs from the computation of the planar fit. When we choose the seven SBAS stations as described in Section 2, the IPPs from those stations are not enough to simulate multiple examples of undersampled threats with a limited set of storm data. Thus, to better represent users under ionospheric irregularity, we employ "oversampling" methodology designed for the MSAS ionospheric threat model [5]. This method uses the IPPs from GEONET stations, a dense GPS observation network in Japan, in addition to those from MSAS reference stations for data deprivation to capture undersampled ionospheric conditions. Similarly we utilize ionospheric delay measurements observed at all 74 GNSS reference stations to simulate as many cases of ionospheric irregularities as possible.

A threat model is constructed as follows. To determine $\sigma^2_{undersampled}$, the augmentation of the GIVE variance required to protect against undersampling, we compute the maximum error associated with undersampled irregularities, as given in Equation (1) [3][12].

$$\sigma^{raw}_{undersmapled}(R_{fit}, RCM) = \max_{over\ k,T}\left[\sqrt{\frac{\left|\bar{I}_k - \tilde{I}_k\right|^2}{K^2_{undersampled}} - \tilde{\sigma}^2_k}\right] \quad (1)$$

$\bar{I}_k$ is a measured slant ionospheric delay projected to vertical at the k^{th} Ionospheric Pierce Point (IPP). This precise delay measurement is obtained from the simplified truth processing method described in [6-8]. $\tilde{I}_k$ is the corresponding vertical delay estimate at the k^{th} IPP derived from a planar fit [10]. $K_{undersampled}$ is a constant that translates the maximum residual into a one-sigma value of a Gaussian distribution [3], and $\tilde{\sigma}_k$ is the inflated formal error variance of the delay estimate at the IPP [12]. The raw data are tabulated in the threat model as a function of threat model metrics that are the planar fit radius, R_{fit}, and the Relative Centroid Metric, *RCM*, the ratio of the centroid radius to the fit radius. These are originally introduced as metrics of the WAAS ionospheric threat model to provide a measure of the density or uniformity of IPPs in the region around each IGP.

3.2 Modification of IPP Selection Parameters

The original IPP search algorithm used in WAAS and MSAS defines IPP selection parameters: R_{min} = 800 km, R_{max} = 2100 km, N_{target} = 30, and N_{min} = 10. R_{min} and R_{max} define a circular area within which a radial search, centered at the IGP, is performed [3][11]. N_{target} is the targeted number of IPPs desired to perform planar fitting, and N_{min} is the minimum number of IPPs required for the fitting. If IPPs fewer than N_{min} are within the maximum search radius (i.e., R_{max}), the GIVE for that IGP is set to "Not Monitored" [3]. When N_{target} of 30 are found within R_{max}, either the distance in kilometers from the IGP to the most distant IPP or R_{min} is simply used as the fit radius.

When compared to the cases of WAAS or MSAS, a wide distribution of reference stations is difficult in the Korean region due to the limited territory. For this reason narrowly distributed IPP geometries can occur frequently in the Korean region. Thus, to acquire the targeted number of IPPs of 30, the fit radius needs to be extended further than the cases of the WAAS or MSAS. In this procedure, extending the fit radius excessively degrades the quality of the planar fit. Thus, we modify the criteria of IPP selection parameters that are used to select IPPs for the planar fit algorithm.

In this study, the minimum number of IPPs, N_{min}, and the targeted number of IPPs, N_{target}, are set to be 10 and 21 respectively. These criteria are determined through an off-line analysis of the number of IPPs observed at reference stations in South Korea during the period shown in Table 1. We also determined the range of the fit radius within which the number of IPPs from N_{min} to N_{target} is acquired considering the distribution of IPPs in the Korean region. As a result, the minimum fit radius, R_{min}, and the maximum fit radius, R_{max}, are set as 400km and 1600km, respectively. The reduction of selection criteria for N_{target} and the fit radius could decrease observability on ionospheric irregularity undersampled threats due to the insufficient number of IPPs. This can be redeemed by implementing the oversampling method described in Subsection 3.1.

Although the modified IPP selection criteria are applied to the planar fit algorithm, the cases of the number of IPPs less than 21 within the fit domain defined by the modified fit radius may occur frequently in the Korean region. Thus as long as IPP points greater than N_{min} are observed within the fit domain, we use the distance from the IGP to the most distant IPP as the fit radius. This was done to avoid overconservatism that might arise if the current method is applied within the weak IPP condition in the Korean region. The same IPP search algorithm used for the threat model construction is applied to all availability simulations conducted in this study. More details on the availability simulation are described in Section 4.0.

As noted above, the design of threat model metrics is important to avoid an overconservatism of GIVEs and improve system availability. Especially in the Korean peninsula where the IPP coverage of reference stations is limited and the observability at the edge of the service volume is very poor, the reduction of the threat model contribution to GIVE is critical. Thus, in addition to the modification of IPP selection parameters, we propose an alternative threat metric to characterize IPP distributions more effectively for future SBAS in Korean region. The details are described in following subsection.

3.3 New Threat Model Metric: Relative Bin Number (RBN)

The undersampled ionospheric threat model is designed to protect users from the worst case threats by augmenting the confidence bounds with tabulated corrections. The corrections (i.e., error variances) are tabulated as a function of threat model metrics that measure of the sparseness or non-uniformity of IPP distributions around each IGP. In particular, highly skewed IPP distributions and planar fits with large fit radii can occur frequently in the Korean region where a wide distribution of reference stations is difficult. These poor IPP geometries in general require large error variances to be added to GIVE computation. Moreover, the metrics, if poorly designed, may apply worse error variances than needed to less weak IPP geometries [3]. Thus, the threat model metrics that accurately characterize threatening undersampled geometries are essential when seeking to improve the performance of SBAS.

To overcome the limitations of existing metrics (as explained in Section 1.0), a new metric which effectively subdivides the cases of IPP distribution is designed for the Korean SBAS threat model. The *Relative Bin Number* (RBN) metric uses the fit radius, R_{fit}, and the relative bin number, the ratio of the number of empty bins to the total number of bins as a measure of IPP distribution. The first metric, R_{fit}, determines the total area of a circle indicating the boundary that includes the IPPs to be used for the planar fit algorithm. The area of a circle with a radius of R_{fit} is divided by concentric rings inside the circle and evenly distributed lines which penetrate the origin of the circle, forming a shape of dartboard as shown in Figure 2. Note that all the partitions in the circle, here represented as "bins", are equally spaced and each bin has the same area.

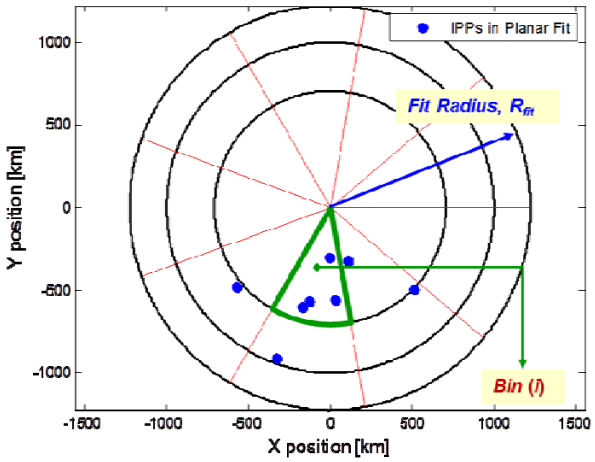

Figure 2. The area within the fit radius (R_{fit}) is divided into equally spaced partitions. The RBN metric determines the skewness of IPP distribution around an IGP considering the number of occupied bins and the IPP density inside the bins as well as uncertainties associated with measurement quality and ionospheric process noise.

The second metric is defined as the ratio of the number of bins in which IPPs do not exist to the total number of bins. Because the RBN measures the ratio of area in which IPPs are absent within the circle, it is superior for capturing the sparseness of the IPP distribution and thus undersampled conditions. The RBN for a given IPP geometry is computed in the following steps. First, the number of bins where IPPs are present, N_{subset} , is counted. However, the uniformity of IPP distributions cannot be measured simply by counting N_{subset} if each bin contains a different number of IPPs as shown in Figure 2. Thus we consider the relative density of IPPs within each bin compared to that of other bins. A bin with higher IPP density is not counted as one bin but a partial bin, since it represents greater IPP skewness. When measuring the relative IPP density of each bin, we also need to consider the quality of measurement at IPPs. The IPPs with poor measurements are less weighted in planar fit, and thus the same is done for RBN computation. The inverse of the relative IPP density, D_{inv}, of the K^{th} bin is expressed as

$$D_{inv}(k) = \frac{N_{IPP\_total}}{N_{IPP\_LW}(k)}; \quad k = 1, 2, \ldots, N_{subset}; \tag{2}$$

$$N_{IPP\_LW}(k) = \frac{1}{\max\limits_{j=1,\ldots,N_{IPP}(k)} \left(1/\sigma_j^2\right)} \sum_{j=1}^{N_{IPP}(k)} \left(1/\sigma_j^2\right); \quad (3)$$
$$j = 1, 2, \ldots, N_{IPP}(k);$$

where $N_{IPP}(k)$ is the number of IPPs in the k^{th} subset (i.e. the bin), and N_{IPP_total} is the total number of IPPs within the planar fit radius.

The effective number of IPPs in the k^{th} subset, $N_{IPP\_LW}(k)$, is counted by applying a locally scaled weight to each IPP. The measurement uncertainty at the j^{th} IPP, σ_j^2, is given by Equation (4):

$$\sigma^2 = \sigma_{IPP}^2 + \sigma_{decorr}^2 \quad (4)$$

where σ_{IPP}^2 is the measurement noise variance of ionospheric delay at the j^{th} IPP and σ_{decorr}^2 is the delay variance of ionospheric decorrelation [10]. This locally weighted number of IPPs is computed by combining the ratios of the $1/\sigma^2$ assigned to each IPP to the maximum $1/\sigma^2$ among all IPPs within the bin.

To estimate the contribution of each bin to non-uniformity of IPP distribution, the IPPs are weighted locally so far based on the local maximum value of $1/\sigma^2$. Now to count the effective number of occupied bins adjusted by the measurement quality at IPPs, each bin is globally weighted again by the sum of $1/\sigma^2$ of IPPs within each bin. This weighted bin number, C, is given in Equation (5), and finally the RBN metric is calculated as shown in Equation (6).

$$C = \sum_{k=1}^{N_{Subset}} \left[\left(\frac{\sum_{j=1}^{N_{IPP}(k)} 1/\sigma_j^2}{\sum_{i=1}^{N_{IPP\_total}} 1/\sigma_i^2} \right) \cdot D_{inv}(k) \right]; \quad (5)$$
$$i = 1, 2, \ldots, N_{IPP\_total};$$

$$RBN = \frac{N_{bin\_total} - C}{N_{bin\_total}} \quad (6)$$

where N_{bin_total} is the total number of bins, which is 21 as a default and is determined according to the targeted number of IPPs to be used for the planar fit algorithm.

3.4 Results: Ionospheric Irregularity Threat Model for SBAS in Korean Region

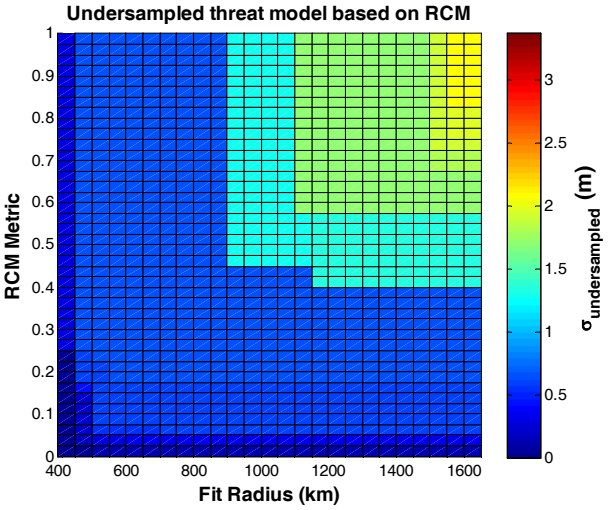

(a)

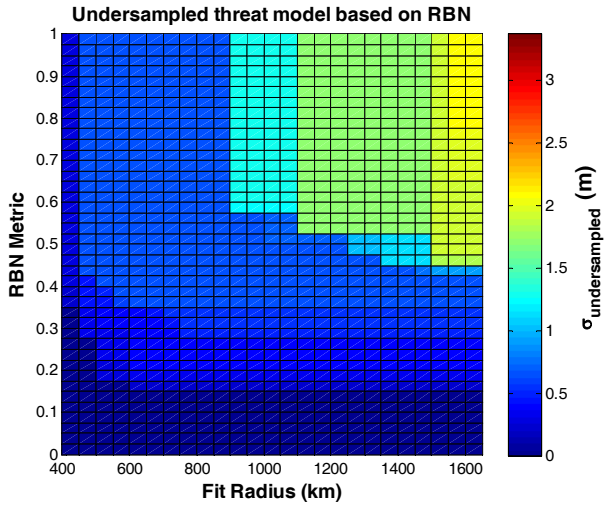

(b)

Figure 3. a) Undersampled ionospheric irregularity threat model derived by the RCM metric. b) Threat model constructed by the newly proposed RBN metric. The RBN metric better distinguishes good IPP geometries from poor IPP geometries.

In this subsection, we present an undersampled ionospheric irregularity threat model for SBAS in the Korean region, constructed from applying the methodologies described in the previous subsections. Multiple threats are tabulated into the threat model by applying the same deprivation schemes employed in the WAAS threat model and the oversampling method developed for the MSAS threat model. These methodologies require determining several parameters used to select IPPs in planar fit [11]. Thus, we analyzed the IPP distribution observed at GNSS reference stations

in South Korea during the period of 2000-2004 to determine the suitable parameters for the IPP search algorithm as described in Subsection 3.2. The IPP selection parameters and criteria determined are as follows: R_{min} = 400 km, R_{max} = 1600 km, N_{target} = 21, and N_{min} = 10.

The upper plot of Figure 3 shows the resulting threat model derived as a function of the RCM metric. The lower plot shows the threat model constructed as a function of the RBN metric. These resulting threat models are derived by employing a monotonic overbound logic to $\sigma^{raw}_{undersampled}$ calculated from Equation (1) [3]. For the case of the RBN based threat model, the magnitudes of $\sigma_{undersampled}$ are decreased in the threat regions of good geometry, compared to those of the RCM based model. In particular, we see a significant reduction of $\sigma_{undersampled}$ in the region below 0.5 RBN. This indicates that the proposed RBN metric works well in distinguishing good IPP geometries from poor geometries compared to the RCM metric and consequently keeps the magnitude of $\sigma_{undersampled}$ low for good IPP geometries.

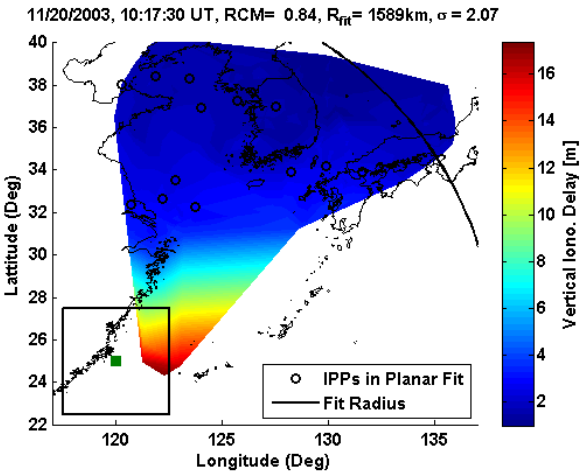

Figure 4. The worst undersampled ionospheric threat was observed during the November 20, 2003 storm.

The largest magnitude of $\sigma_{undersampled}$ tabulated in the threat model in both (a) and (b) of Figure 3 reaches up to about 2 m which was observed from the November 20, 2003 storm. Figure 4 shows the worst undersampled ionospheric threat to the system observed during 2000-2004 in the Korean region. In Figure 4, the green square at the left bottom corner indicates an IGP and the box centered at the IGP denotes a region within which virtual user IPPs contribute to the deviations shown in the threat model. As mentioned earlier, the narrow distribution of reference stations in South Korea often results in highly skewed IPP geometries. These skewed IPP geometries result in absence of IPPs in the region where ionospheric irregularities exist (i.e., the box in Figure 4), and consequently high magnitudes of $\sigma_{undersampled}$. In this case, RCM is 0.84 and the fit radius is 1589km (which is very close to the predefined maximum fit radius).

4.0 AVAILABILITY SIMULATION

To examine the performance of the threat model developed in Section 3.0, we conduct SBAS availability simulations in the Korean region. The baseline conditions of IGP formation and UDRE computation are described in Subsection 4.1 and 4.2 respectively. The simulations presented in this paper are performed using the MAAST (Matlab Algorithm Availability Simulation Tool) developed at Stanford University [13].

4.1 IGP and User Grid Formation

Figure 5 shows the IGP formation (denoted as green dots) used for the availability simulation. The five-by-five degree IGP formation was derived from shifting the MSAS IGP formation leftward by 10 degrees to cover all IPPs within the IGP formation. A 0.5-by-0.5 degree rectangular grid is used as user location to calculate time availability at specific locations. As for availability coverage, the fraction of users within specified regions where time availability is greater than or equal to a given availability performance is calculated [13]. In this study, all coverage simulations are conducted for the availability of 99.9% and the results are shown in Section 4.3.

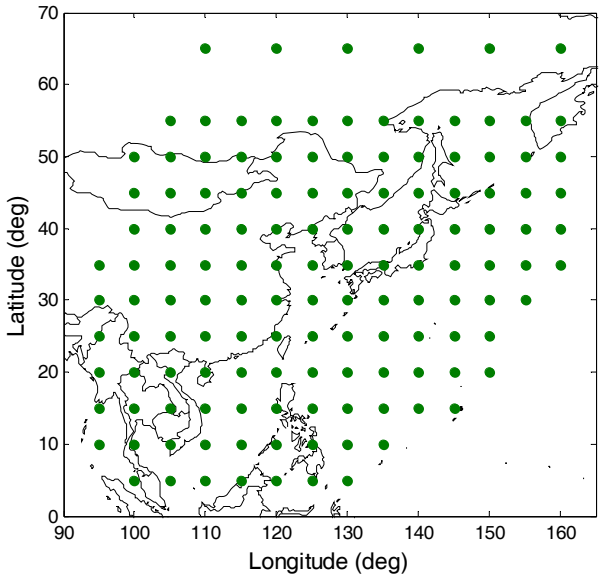

Figure 5. Ionospheric Grid Point (IGP) formation used for availability simulation (green dots).

4.2 GEO Message Type 28

In addition to GIVE, SBAS monitors and broadcasts UDRE (the User Differential Range Error), to bound the user range error due to satellite clock and ephemeris errors. UDRE is a single scalar confidence bound. Thus, UDRE originally needs to be the largest projected value applicable for all users. To avoid such over-conservatism on UDRE, MT28 (Message Type 28) is applied to specify the correction confidence as a function of the specific user location [14]. The user calculates $\delta UDRE$ with MT28 and inflates the given UDRE to obtain the integrity bound. In Equation (7), the clock and ephemeris error bound is calculated by multiplying the broadcasted UDRE and $\delta UDRE$, which is the UDRE inflation factor for each user location.

$$\sigma_{flt}^2 = \sigma_{UDRE}^2 \times \delta UDRE \tag{7}$$

where σ_{flt}^2 is the error variance associated with satellite clock and ephemeris errors, and σ_{UDRE}^2 is the broadcast UDRE. MT28 is determined as a function of the satellite and monitoring station geometry. GPS MT28 continuously varies because GPS satellites are orbiting. In contrast, GEO MT28 is a fixed matrix given that the geometry between GEO and the SBAS reference stations does not change and thus GEO broadcasts a fixed MT28 message. In this paper, we determined a fixed GEO MT28 matrix for availability simulation. The computation process used for GPS MT28 [14] is applied under the assumption that the GEO satellite is at the longitude of 127 deg. and the latitude of 0 deg. The longitude of GEO was determined to cross the center of South Korea.

4.3 Simulation Results

Availability simulations were conducted using three threat models constructed using the different combinations of threat model metrics and IPP selection parameters: RCM metric and IPP selection parameters used in WAAS, RCM metric and IPP selection parameters adjusted for SBAS in the Korean region, and RBN metric and the adjusted IPP selection parameters. The results were assessed for Approach operation with Vertical guidance (APV)-I service, for which Horizontal Alert Limit (HAL) is equal to 40 meters and Vertical Alert Limit (VAL) is equal to 50 meters.

The first case assesses the availability of the future SBAS in Korean region when an ionospheric threat model is developed using the existing methodologies employed for WAAS and the oversampling scheme for MSAS (see Section 3.1). In this case, we used the RCM metric, the planar fit method and the same IPP selection parameters applied for the WAAS threat model: R_{min} = 800 km, R_{max} = 2100 km, N_{target} = 30, and N_{min} = 10. Figure 6a shows the resulting ionospheric undersampled irregularity threat model and Figure 6b displays the simulation result of the APV-I service availability. The coverage of 99.9% availability for APV-I service is only 18.48% in South Korea. Therefore, if we apply the ionospheric threat model derived by the existing planar fit algorithm, IPP selection parameters, and RCM threat metric being used for WAAS and MSAS to the GIVE algorithm of a future Korean SBAS, the system performance is very poor for providing the service of vertical guidance flight modes.

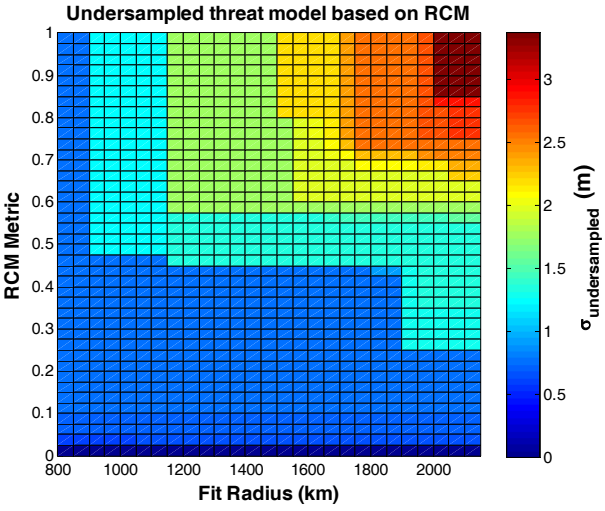

(a)

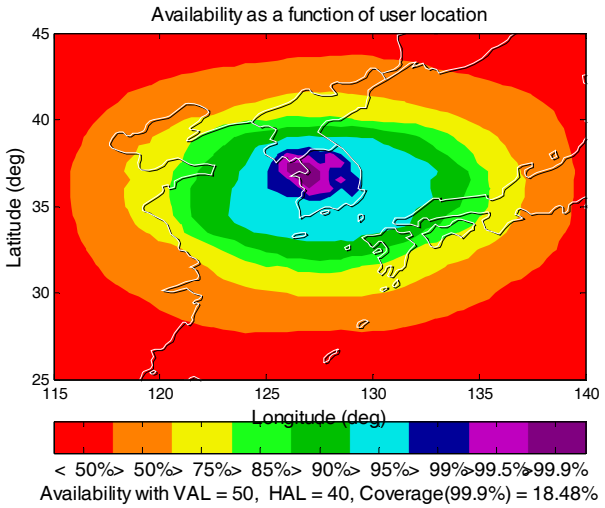

(b)

Figure 6. a) Undersampled ionospheric threat model based on RCM metric using the same methodologies and IPP selection parameters used for WAAS threat model. b) Availability for APV-I service in the Korean region when the threat model shown in (a) is applied to the GIVE algorithm.

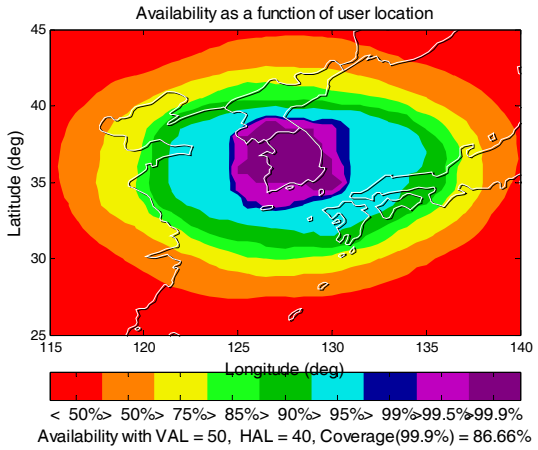

(a)

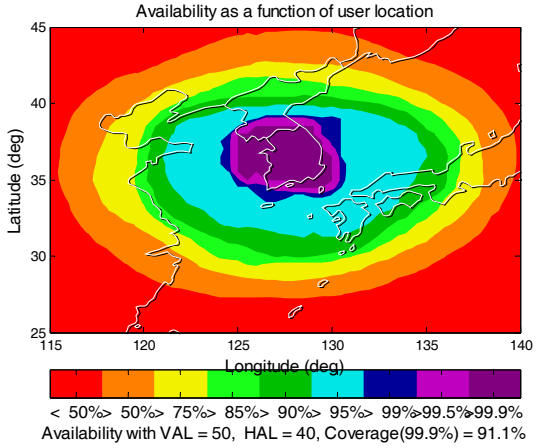

(b)

Figure 7. SBAS availability assessment for APV-I service in the Korean region with undersampled threat models based on RCM metric (a) and RBN metric (b). Differing from the case of Figure 6, IPP selection criteria were adjusted for the Korean region.

The availability results for two other cases were obtained by applying newly derived ionospheric threat models (shown in Figure 3) based on the RCM metric and the RBN metric, respectively. As for the previous simulation in Figure 6, the same planar fit algorithm and deprivation methods are applied. However, as discussed in Subsection 3.2, the IPP selection parameters suitable for the Korean region are predetermined and used in the threat model development and availability assessment. Figure 7a shows the AVP-I service availability when the ionospheric threat model based on the RCM metric is applied to the GIVE algorithm. Because location-specific conditions are considered to choose the parameters for the IPP search algorithm, the availability performance is increased dramatically (i.e., by about 68%), compared to that shown in Figure 6. The coverage of 99.9% availability for APV-I service is now 86.66%, but yet needs to be increased further.

Figure 7b presents the result for APV-I service when the ionospheric threat model constructed based on the proposed RBN metric is applied to the GIVE algorithm. The coverage of 99.9% availability for APV-I service is increased from 86.66% to 91.10% (by about 4.4%). In addition, the regions of achieving 95% or less availability are increased. This result demonstrates the performance of the RBN based threat model is better than the RCM based model in reducing the threat model contribution to GIVE values. However, in Figure 7b, the performance is not yet enough to provide vertical guidance in the southernmost part of the land and the Jeju island.

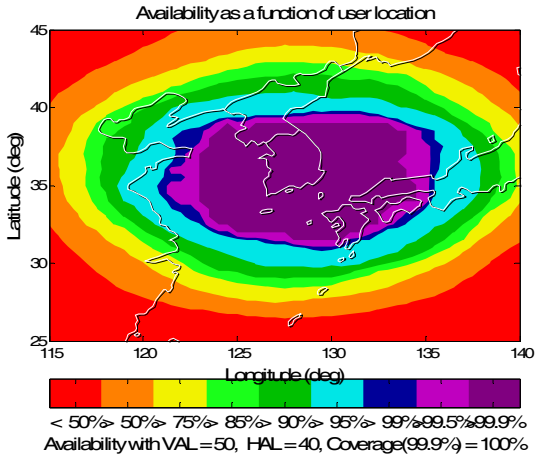

Figure 8. SBAS availability assessment for APV-I service in the Korean region with two hypothetical stations surrounding South Korea added to the seven candidates of SBAS reference stations. The addition of the two stations (shown in Figure 9) improves system availability to a great extent.

We also investigated how the number and location of SBAS reference stations affect the performance of system availability. The RBN-based ionospheric threat model is again applied to the GIVE algorithm in the simulation. Figure 9 displays the configuration of 9 reference stations (seven predefined monitor stations and additional two hypothetical stations - one in Japan and the other in China). As expected, additional reference stations provide better IPP distribution and ionospheric observability, and thus the availability performance improves significantly as shown in Figure 8. Thus the optimized number and formation of SBAS reference stations is also essential components to be considered for system design of a future Korean SBAS.

The GIVE value, whose dominant contribution usually comes from the ionospheric threat model, is one of key parameters to determine the magnitude of the user Vertical Protection Level (VPL). The benefits of implementing a new threat model and configuring a wider

station network are demonstrated in this study. However, a desired availability performance for APV-I service is not yet achieved. Thus, further studies pertaining to reduce the GIVE values, including the methodologies for undersampled threat model, ionospheric algorithms, and the number and formation of SBAS reference stations, are needed to improve system availability.

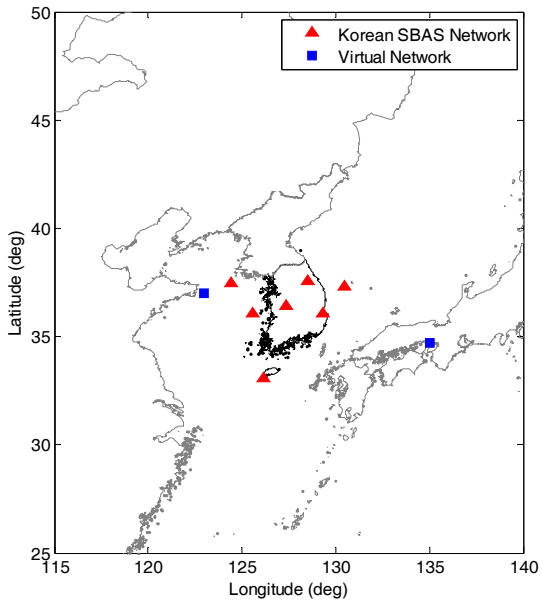

Figure 9. Configuration of SBAS reference stations: seven predefined candidates (red triangles) and a hypothetical network (as blue squares) added for availability simulation.

5.0 CONCLUSION

In this paper, we present an undersampled ionospheric irregularity threat model for SBAS in the Korean region, constructed using newly proposed methodologies. In addition, we demonstrate the performance of the undersampled threat model by conducting a preliminary assessment of the single-frequency based SBAS availability in the Korean region. As a result, it is found that improvement of the availability in the Korean region can be achieved by applying the undersampled threat model derived using the modified methodologies to the GIVE algorithm of a future Korean system. In particular, total improvement of 72.6% is achieved using the modified IPP selection parameters and the RBN metric. The benefits of using the RBN metric is expected to be greater when applied to the system with a good configuration of reference stations, similar to the case of WAAS.

We also investigated how the number of SBAS reference stations affects the system availability. Further studies on the number and location of the reference stations, ionospheric algorithms, threat metrics, optimized parameters for IPP search algorithm, and additional GEO are needed to provide better system performance to users. This work would help with the design of the Korean SBAS architecture if deployed in the future.

ACKNOWLEDGMENTS

The authors thank Per Enge, Sam Pullen, and Juan Blanch of Stanford for their support of this work. Eugene Bang was supported by Basic Science Research Program through the National Research Foundation of Korea (NRF) funded by the Ministry of Education, Science and Technology (2012-0007550). Jinsil Lee was supported by the KAIST Institute. Jiwon Seo was supported by the Ministry of Knowledge Economy (MKE), Korea, under the “IT Consilience Creative Program” support program supervised by the National IT Industry Promotion Agency (NIPA) (NIPA-2012-H0201-12-1001).

REFERENCES

[1] Sparks, L., Komjathy, A., Manucci, A., “Extreme Ionospheric Storms and Their Impact on WAAS,” *Proceedings of the Ionospheric Effect Symposium 2005*, Alexandria, VA, May 2005.

[2] Walter, T., et al., “Protecting Against Unsampled Ionospheric Threats,” *Proceeding of the International Beacon Satellite Symposium 2001*, Trieste, Italy, October 2004.

[3] Pandya, N., Gran, M., Paredes, E., "WAAS Performance Improvement with a New Undersampled Ionospheric Gradient Threat Model Metric," *Proceedings of the 2007 National Technical Meeting of The Institute of Navigation*, San Diego, CA, January 2007, pp. 291-304.

[4] Altshuler, Eric S., et al., "The WAAS Ionospheric Spatial Threat Model," *Proceedings of the 14th International Technical Meeting of the Satellite Division of The Institute of Navigation (ION GPS 2001)*, Salt Lake City, UT, September 2001, pp. 2463-2467.

[5] Sakai, T., et al., “Modeling Ionospheric Spatial Threat Based on Dense Observation Datasets for MSAS," *Proceedings of the 21st International Technical Meeting of the Satellite Division of the Institute of Navigation (ION GNSS 2008)*, Savannah, GA, September 2008, pp. 1918-1928.

[6] Lee, J., Jung, S., Bang, E., Pullen, S., Enge, P., "Long Term Monitoring of Ionospheric Anomalies to Support the Local Area Augmentation System," *Proceedings of the 23rd International Technical Meeting of The Satellite Division of the Institute of Navigation (ION GNSS 2010)*, Portland, OR, September 2010, pp. 2651-2660.

[7] Lee, J., Jung, S., Pullen, S., "Enhancements of Long Term Ionospheric Anomaly Monitoring for the Ground-Based Augmentation System," *Proceedings of the 2011 International Technical Meeting of The Institute of Navigation*, San Diego, CA, January 2011, pp. 930-941.

[8] Jung, S., and J. Lee (2012), Long-term ionospheric anomaly monitoring for ground based augmentation systems, Radio Sci., 47, RS4006, doi:10.1029/2012RS005016.

[9] DGPS CENTRAL OFFICE, "Reference and Monitor stations," https://www.ndgps.go.kr [retrieved 1 March 2013].

[10] Walter, T., A. Hansen, J. Blanch, et al., "Robust Detection of Ionospheric Irregularities," *Proceedings of the 13th International Technical Meeting of the Satellite Division of The Institute of Navigation (ION GPS 2000)*, Salt Lake City, Utah, 19-22 September 2000, p. 209-218.

[11] Sparks, L., J. Blanch, and N. Pandya (2011), Estimating ionospheric delay using kriging: 1. Methodology, Radio Sci., 46, RS0D21, doi:10.1029/2011RS004667.

[12] Sparks, L., J. Blanch, and N. Pandya (2011), Estimating ionospheric delay using kriging: 2. Impact on satellite-based augmentation system availability, Radio Sci., 46, RS0D22, doi:10.1029/2011RS004781

[13] Jan, Shau-Shiun., et al., "Matlab Simulation Toolset for SBAS Availability Analysis," *Proceedings of the 14th International Technical Meeting of the Satellite Division of The Institute of Navigation (ION GPS 2001)*, Salt Lake City, UT, September 2001, pp. 2366-2375.

[14] Walter, T., et al., "Message Type 28," *Proceedings of the 2001 National Technical Meeting of The Institute of Navigation*, Long Beach, CA, January 2001, pp. 522-532.